Contribution from the Biomedical Chemistry Research Center and Department of Chemistry, University of Cincinnati, Cincinnati, Ohio 45221-0172, and Department of Chemistry, New Mexico State University, Las Cruces, New Mexico 88003

Determination of Gold Binding in an Algal Biomass Using EXAFS and XANES Spectroscopies

J. W. Watkins II,[†] R. C. Elder,*[†] Benjamin Greene,[‡] and Dennis W. Darnall[‡]

Received April 18, 1986

The alga *Chlorella vulgaris* has been shown to have a high affinity for both gold(I) and gold(III) species in aqueous solutions. The accumulation of gold may approach 10% or more of the algae dry weight. We have used X-ray absorption spectroscopy to investigate Au–algae samples prepared from aqueous solutions of the antiarthritic drug Myochrisine (sodium gold(I) thiomalate) and the gold complexes dicyanoaurate(I) and tetrachloroaurate(III). The oxidation state of the algae-bound gold and the structure of the gold coordination sphere that results upon binding have been determined. These results indicate that chemical reaction, not simply electrostatic interaction, is involved in the binding of the gold to the algae. The predominant oxidation state in algae complexes is Au(I). For samples derived from Au(I) complexes, the ligating atom appears to be sulfur while, for the samples prepared from Au(III), the product appears to bind Au(I) to a nitrogen moiety.

Introduction

Biomass, prepared from algal, fungal, or bacterial cells, has been shown to be an efficient binding medium for transition-metal ions.[1] Our interest in these systems arose from the recent finding that gold binds to algal biomass.[2,3] Under certain conditions, gold bound to algae accounts for up to 10% dry weight. Moreover gold is efficiently and reversibly bound to the algal biomass from solutions with concentrations of gold as low as 10^{-9} M. Since this biomass is both relatively inexpensive and easy to prepare, this process may provide a lucrative method for recovery of precious metals from mining effluents as well as lead to other industrial applications.[3]

Biosorption, in which metal complex ions interact with the functional groups on the surface or within the cellular matrix of the binding material, can occur via a substitution process in which a ligand bound to the metal is replaced by a ligating moiety from the algae. Binding may also occur from the interaction of the charged metal complexes with charged or polar functional groups on the algae. We refer to the former process as complexation and the latter process as electrostatic binding. Lipophilic interactions, wherein the metal is already complexed by lipophilic ligands and partitions into the fatty cellular matrix of the biomass, may also account for some of the binding. The biosorption process may occur with either living or dead organisms.

Prepared biomass from the alga *Chlorella vulgaris* was used as the standard binding material in our experiments. Like any cellular material, the biomass prepared from *C. vulgaris* is chemically complex. Any or all of the proposed binding modes may be involved in such a system. We wished to determine not only the mode of binding in the algae samples but also the oxidation state of the gold species bound to the algae, especially when the starting material contains gold in the +3 oxidation state. This is because we have some evidence from UV–vis spectroscopy that, upon binding to algae, gold(III) is rapidly reduced to gold(I) and then eventually to gold(0).[4] We used X-ray absorption spectroscopy to investigate the binding of three gold complexes. The first is sodium gold(I) thiomalate, Myochrisine, which is used as an injectable drug for the treatment of rheumatoid arthritis. The second complex is potassium dicyanoaurate(I), another gold(I) species, and the third, tetrachloroaurate(III), was chosen as a representative gold(III) species. We measured both the X-ray absorption near-edge structure (XANES), to determine information on the oxidation state of the bound gold in the samples, and the extended X-ray absorption fine structure (EXAFS), to determine information about the type and number of atoms bound to gold and their distances from gold, and report those results here.

Experimental Section

Preparation of Au–Algae Samples. The alga *C. vulgaris* was cultivated in a New Brunswick fermentation apparatus. The growth medium consisted of Bold's basic medium where the pH was maintained near 6.5 with sodium carbonate and hydrochloric acid. The algae were harvested with a Sharples continuous-flow centrifuge and lyophilized. The final material was a fine, green powder, which was stored at −20 °C until used for sample preparation.[5]

Aqueous stock solutions of the gold complexes were prepared from potassium dicyanoaurate(I), hydrogen tetrachloroaurate(III) (Strem Chemicals, Inc.), and sodium gold(I) thiomalate, AuSTm, (injectable form, Merck Sharpe & Dohme). The solutions were each adjusted to pH 3.0 by the addition of nitric acid before incubation with algae.

The lyophilized algae were suspended in an aqueous solution of the same pH as the gold-containing solution, agitated, and centrifuged three times to remove extracellular or algal-derived biomolecules that could be solubilized. The washed algae were then suspended in the desired gold-containing solution and agitated for 30 min. The reaction mixture was centrifuged (4 min, 2500 rpm) and the supernatant saved for analysis. The algae were then washed twice with a pH 3.0 HNO_3 solution. The amount of gold accumulated in the algae was determined by the decrease in free gold concentration in the solution or by the digestion of the algae cells in aqua regia. The gold analyses were performed by using atomic absorption spectroscopy measured with an Instrument Laboratory 457 spectrometer. The incubation process can be repeated on a given algae sample until saturation occurs with a gold content of ca. 10% of the algae, dry weight. Algal–gold samples were prepared that contained different amounts of bound gold. The samples were lyophilized immediately after preparation and subsequently characterized by X-ray analysis. The final gold contents of the algae samples, in percent by dry weight of the algae, are as follows: from the reaction of AuSTm and the algae, the samples contained 8.7%, 1.0%, and 0.1% gold by weight; from $Au(CN)_2^-$, the samples contained 1.4% and 0.08% gold; from $AuCl_4^-$ the samples contained 7.5% and 0.1% gold.

EXAFS/XANES Data Collection and Analysis. X-ray absorption spectra were collected at the Stanford Synchrotron Radiation Laboratory on beam line IV-1. Lyophilized Au–algae samples were packed in aluminum sample holders with an approximate sample dimension 28 mm long × 3 mm high × 0.5 mm thick. A fluorescence detector[6] (EXAFS Co., Seattle, WA) with a germanium filter to discriminate against scattered radiation was used for the measurement of Au Lα fluorescence. X-ray spectra were recorded in the range 11 900–11 980 eV for the XANES analysis and 11 500–13 000 eV for the EXAFS analysis, with both ranges encompassing the Au L_{III} absorption edge. XANES spectra were recorded for all of the samples; however, EXAFS scans were collected for the samples derived from AuSTm, the 1.4% Au and 0.08% Au samples derived from $Au(CN)_2^-$, and the 7.5% Au sample derived from $AuCl_4^-$. Energy calibration of the data was achieved by the simultaneous

[†] University of Cincinnati.
[‡] New Mexico State University.

(1) Hassett, J. M.; Jennett, J. C.; Smith, J. E. In *Contaminants and Sediments*; Baker, R. A., Ed.; Ann Arbor Science: Ann Arbor, MI, 1980.
(2) Greene, B.; Darnall, D. W.; Alexander, M. D.; Henzl, M. T.; Hosea, J. M.; McPherson, R. A. *Abstracts of Papers*, 190th National Meeting of the American Chemical Society, Chicago, IL; American Chemical Society: Washington, DC, 1985; GEOC 86.
(3) Darnall, D. W.; Greene, B.; Henzl, M. T.; Hosea, J. M.; McPherson, R. A.; Sneddon, J.; Alexander, M. D. *Environ. Sci. Technol.* **1986**, *20*, 206.
(4) Greene, B.; Hosea, M.; McPherson, R.; Henzl, M.; Alexander, M. D.; Darnall, D. W. *Environ. Sci. Technol.* **1986**, *20*, 627.
(5) James, D. E. *Culturing Algae*; Carolina Biological Supply Co.: Burlington, NC, 1978.
(6) Stearn, E. A.; Heald, S. M. *Rev. Sci. Instrum.* **1979**, *50*, 1579.

0020-1669/87/1326-1147$01.50/0

Table I

incubation compd	% Au in algae	inflection point energy, eV	peak position energy, eV
AuSTm	solid[a]	11921.8	
	8.7	11921.7	
	1.0	11922.2	
	0.1	11922.1	
$Au(CN)_2^-$	solid	11923.8	11928
	1.4	11923.8	11928
	0.08	11923.3	11928
$AuCl_4^-$	solid	11919.2	11923
	7.5	11920.6	11923
	0.1	11921.8	

[a] This measurement is for the pure compound with no algae present.

measurement of the Au foil absorption spectrum with a known inflection point energy of 11921.2 eV. For the EXAFS scans, a total of 220 data points were collected beyond the edge at evenly spaced intervals in **k** space. Integration times varied from 1 to 12 s/point, the longer time being used for the points farther from the edge. Two to four scans were collected per sample and then averaged together for analysis.

The details of the XANES and EXAFS data analysis procedure have been published previously.[7,8] The EXAFS data were extracted from the fluorescence measurements by following our standard method. Typically, a k range of 3–13 $Å^{-1}$ was used for the Fourier transformation. We define **k** equal to zero at 11940 eV. From the Fourier transform, an R range, in Å space, was chosen to encompass the frequency component(s) of interest for back-transformation to **k** space ($Å^{-1}$). The back-transform, weighted by k^3, is used for curve fitting analysis over a k range of 4–12 $Å^{-1}$. Model compounds used for the empirical curve fitting for the determination of the absorber–scatterer bond lengths and coordination numbers are as follows: $(etu)_2Au^I Cl{\cdot}H_2O$ [etu = ethylenethiourea], with a crystallographically determined[9] Au–S distance of 2.276 Å; $[P(C_6H_6)_4](AuCl_4)$, with a crystallographically determined[10] Au–Cl distance of 2.285 Å; $[Au(NH_3)_4](NO_3)_3$, with a crystallographically determined[11] Au(I)–N distance of 2.02 Å; $KAu(CN)_2$, with estimated distances for Au(I)–C being 2.00 Å and for Au(I)–N being 3.14 Å. The distance estimate is from the crystallographic values for the salt $K_5[Au(CN)_2]_4[Au(CN)_2(I)_2]$.[12]

Results

XANES. The XANES region of the spectrum for the Au–algae samples was examined to extract information regarding the oxidation state of the gold in each sample. In general there are two indications of the Au oxidation state: the inflection point energy of the edge rise and the presence of bound-state peaks in the spectrum. The inflection point energy for Au(0) is established as 11921.2 eV.[13] From a systematic investigation of many gold compounds of known oxidation state,[14] we have found that Au(I) inflection point values occur typically in the range 11921.7–11923.8 eV whereas Au(III) inflection point values occur at the lower energy range 11919.2–11920.0 eV. The lower energy range for Au(III) species results from a lower energy 2p to 5d transition that precedes the excitation to the continuum. Au(III) has a d^8 electron configuration, making this electronic transition possible. Both Au(0) and Au(I) are d^{10} systems; thus, the 2p to 5d transition cannot occur.

Table I lists the inflection points found for the Au–algae samples studied. For those derived from AuSTm and $Au(CN)_2^-$, all of the inflection points are indicative of gold in the +1 oxidation state. For all of the samples derived from $AuCl_4^-$, the inflection point energy is higher than the range found for Au(III). For the $AuCl_4^-$ sample with the least amount of gold bound to the algae, the inflection point energy approaches that of a typical Au(I) system. For the sample with the highest concentration of gold from $AuCl_4^-$, 7.5%, the inflection point occurs at 11920.6 eV. This indicates a mixture of Au(III) and Au(I) species, which gives rise to the intermediate inflection point value. This value, occurring essentially midway between the inflection point energy of 11919.2 for $Au(III)Cl_4^-$ solid and 11921.8 eV for the gold(I) thiomalate solid, suggests that approximately 50% of the Au(III) has been reduced to Au(I).

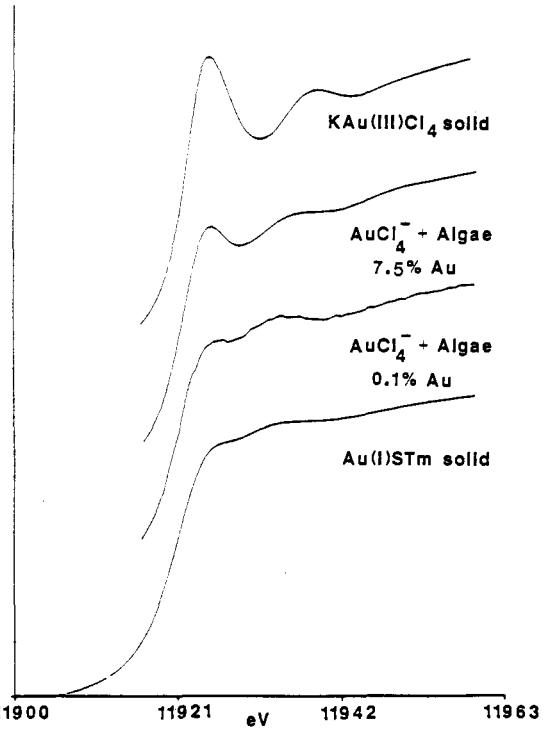

Figure 1. Plots of the XANES region spectra, F/I_0, vs. energy (eV) obtained for solid $KAuCl_4$ with no algae present, the samples derived from the reaction of $AuCl_4^-$ with algal biomass (7.5% and 0.1% Au, respectively) and an example of an Au(I) XANES spectrum taken from AuSTm. The intense band at 11923 eV is characteristic of the Au(III) oxidation state. Energies of edge-rise inflection points are given in Table I.

We confirmed the gold oxidation state in the Au–algae samples by examining the XANES region of the spectrum for peaks that are characteristic of oxidation state. In general, Au(0) exhibits two peaks in the XANES spectrum near 11945 and 11967 eV whereas Au(III) exhibits a single, intense peak near 11922 eV attributed to the 2p to 5d transition. Au(I) is characterized by the lack of such peaks in the XANES region. Table I also lists the energy of any peaks observed in the XANES spectrum. Figure 1 is a plot of the XANES region for solid $AuCl_4^-$ and the corresponding Au–algae samples. The XANES spectrum may also exhibit a peak that is a result of the bonding of certain ligands to the Au(I) species, specifically phosphorus and cyanide. For such systems, an intense peak is observed in the XANES spectrum at ca. 11928 eV. It has been suggested that this peak results from a bound-state transition to an unoccupied molecular orbital.[15] It is readily distinguished from the peak associated with the Au(III) 2p to 5d transition by the difference in their energies. This peak is present for all of the Au–algae samples that were derived from the $Au(CN)_2^-$ starting material.

EXAFS. The EXAFS region of each spectrum was Fourier transformed from **k** space ($Å^{-1}$) to radial space (Å), to visualize the absorber–scatterer pair interactions. Then the desired frequency component(s), represented as a peak or peaks in the Fourier transform, was back-transformed through a Fourier filter to provide the filtered EXAFS for the empirical curve fitting analysis.

(7) Shaw, C. F., III; Schaeffer, N. A.; Elder, R. C.; Eidsness, M. K.; Trooster, J. M.; Calis, G. H. M. *J. Am. Chem. Soc.* **1984**, *106*, 3511.
(8) Elder, R. C.; Watkins, J. W., II. *Inorg. Chem.* **1986**, *25*, 223.
(9) Jones, P. G.; Guy, J. J.; Sheldrick, G. M. *Acta. Crystallogr., Sect. B: Struct. Crystallogr. Cryst. Chem.* **1976**, *32*, 3321.
(10) Elder, R. C.; Ragle, H.; Eidsness, M. K.; Watkins, J. W., II, manuscript in preparation.
(11) Weishaupt, M.; Strahle, J. *Z. Naturforsch., B: Anorg. Chem., Org. Chem.* **1976**, *B31*, 554.
(12) Bertinotti, P. C.; Bertinotti, A. *Acta. Crystallogr. Sect. B: Struct. Crystallogr. Cryst. Chem.* **1972**, *B28*, 2635.
(13) *International Tables for X-ray Crystallography*; Kynoch: Birmingham, England, 1974, Vol. IV, Table 1.1B, p 28.
(14) Eidsness, M. K. Ph.D. Thesis, University of Cincinnati, 1984.
(15) Coffer, M. T.; Shaw, C. F., III; Eidsness, M. K.; Watkins, J. W., II; Elder, R. C. *Inorg. Chem.* **1986**, *25*, 333.

Table II

% Au	model	bond length, Å	coord. no.	fit[a]
		AuSTm		
		Single-Shell Fits		
8.7	S	2.30	1.8	0.13
1.0	S	2.30	2.0	0.18
0.1	S	2.29	2.2	0.32
		Two-Shell Fits		
8.7	S	2.30	1.8	0.12
	N	2.23	0.3	
0.1	S	2.30	2.2	0.28
	N	2.04	0.4	
		$Au(CN)_2^-$		
		Two-Shell Fits		
1.4	C	1.99	1.8	0.46
	N	3.14	2.0	
		Three-Shell Fits		
1.4	C	2.00	2.6	0.20
	N	3.14	2.1	
	S	2.29	0.5	
0.08	C	1.98	2.0	0.54
	N	3.08	0.9	
	S	2.29	1.6	
		$AuCl_4^-$		
		Single-Shell Fits		
7.5	S	2.27	1.6	0.27
7.5	Cl	2.27	1.3	0.40
		Two-Shell Fits		
7.5	S	2.28	1.6	0.08
	N	2.03	0.8	
7.5	Cl	2.29	1.2	0.07
	N	2.05	1.2	

[a] Goodness of fit = $[\sum \mathbf{k}^6((\text{data})\chi)^2/N]^{1/2}$, where N is the number of data points, χ is the calculated EXAFS and $\mathbf{k}$ is the photoelectron wave vector. The lowest value of the function is assumed to give the parameters that best represent the structure. In general, values are only comparable for models using similar curve-fitting $\mathbf{k}$ ranges and the same number of shells.

A combination of single-shell and multishell curve-fitting analyses was used to determine the coordination environment around the gold atom in each of the samples, following techniques we have previously described.[8] Table II summarizes the resulting bond lengths and coordination numbers from the curve-fitting analysis. Plots of the raw EXAFS, Fourier transforms, back-transformed EXAFS, and curve-fit data are available as supplementary material.

Discussion

AuSTm + Algae. The XANES/EXAFS analysis of the samples derived from AuSTm gave conclusive evidence for a gold coordination environment consisting of a Au(I) species bound to two sulfur atoms at a distance of 2.30 (2) Å. A combination of single-shell (using one absorber–scatterer pair such as Au–S) and two-shell (using two absorber–scatterer pairs such as Au–S and Au–N) calculations was used to determine whether, in addition to the expected sulfur coordination, there was any indication of nitrogen, or another light atom such as oxygen, coordinating to gold. Two-shell curve fitting, invoking Au–S and Au–N parameters, does not lead to a significant improvement of the fits obtained over a single-shell Au–S fit, and the gold–sulfur coordination number remains approximately two for both the single-shell Au–S fit and the two-shell Au–S,N fit. The calculated gold–nitrogen coordination number is very small, from 0.3 to 0.4 depending on the sample. We can therefore reject the premise of light-atom coordination, in this sample, on the basis of the vanishingly small Au–N coordination number and the negligible improvement of the fit to the data despite the addition of the Au–N EXAFS parameters. That the Au–S shell consistently yields a calculated coordination number of approximately two confirms a gold atom bound by two sulfur atoms.

Since the gold coordination environment in the AuSTm starting material is the same as that found for these Au–algae samples, it is not possible to distinguish the precise mode of binding (i.e., whether the binding is by gold complexation or electrostatic interaction). It is known, however, that AuSTm binds in other biological systems to free sulfhydryl groups through complexation. We have shown previously that gold binds preferentially to the sulfhydryl site, cysteine-34, in bovine serum albumin (BSA) over other possible sulfur linkages such as thioethers, as in methionein, or disulfides, as in cystine.[7,15] In BSA incubated with AuSTm, low concentrations of gold bind in a 1:1 molar ratio with the albumin, consistent with one gold binding to the single free sulfhydryl residue at cysteine-34. When higher concentrations of AuSTm are incubated with the albumin, up to 7.3 mol of gold are bound per mole of albumin. Apparently one gold complexes to cys-34 and additional gold thiomalate units are bound via sulfur bridges. The bridging nature of thiomalate groups in the starting AuSTm is well documented. The structure of both the amorphous solid AuSTm and a concentrated aqueous solution (approximately 1 M) has been determined by wide-angle X-ray scattering, indicating an open-chain oligomer.[16] In addition, NMR experiments indicate that the extended structure of AuSTm in aqueous solution at pH 3 is expected to consist of a thiomalate-bridged oligomer.[17]

The free sulfhydryl content of a similar batch of algal biomass was found to be 4.3 μmol/g of algae.[4] This is sufficient to account for binding roughly 0.1% Au by dry weight of the algae. Since the AuSTm may be oligomeric in structure, it is possible that more than one gold binds per each sulfhydryl (i.e., one gold bonds directly with the sulfhydryl with the remaining gold atoms linked to the bound gold by bridging thiomalate groups). Even when the oligomeric structure of the AuSTm is taken into account, there are not sufficient sulfhydryl groups to account for all of the gold binding in the concentrated sample. Indeed, the majority of the binding in the 8.7% Au sample must occur by an alternative path, such as the electrostatic interaction of the negatively charged AuSTm units with positively charged sites in the algae.

$Au(CN)_2^-$ + Algae. Unlike the AuSTm case, these samples provide direct evidence for complexation of the Au(I) species with the algae. The change in the coordination sphere is apparent in the Fourier transforms of the EXAFS data. Figure 2a is the Fourier transform (FT) of the data obtained for the starting material $Au(CN)_2^-$. The peaks correspond to absorber–scatterer pairs at a distance that is related to the distance between the absorber–scatterer pair (though phase shifted). Peak 1, at 1.55 Å, is attributed to the Au–C pair, and peak 2, at 2.63 Å, is attributed to the Au–N pair. Notice that the Au–N peak exhibits a magnitude comparable to that of the Au–C peak. Normally the peak intensity decreases as one moves to larger distances; however, in the case of the CN^- ligand, the nitrogen backscattering amplitude function is enhanced by the phenomenon that results from the 180° Au–C–N angle, the well-documented colinearity effect.[18]

Figure 2b is the FT of the data obtained for the 1.4% Au sample. From comparison of the FT here with that for the $Au(CN)_2^-$ starting material, it is evident that there has been a change in the coordination environment about the gold. Peak 1 is associated with the carbon or other light atom coordinated directly to the gold while peaks 3 and 4 are attributed to the nitrogen of the CN ligand.[19] As before, the enhanced amplitude of the Au–N

(16) Elder, R. C.; Ludwig, K.; Cooper, J. N.; Eidsness, M. K. *J. Am. Chem. Soc.* **1985**, *107*, 5024.
(17) Isab, A. A.; Sadler, P. J. J. *Chem. Soc. Dalton Trans.* **1981**, 1657.
(18) Teo, B. K. *J. Am. Chem. Soc.* **1981**, *103*, 3990.
(19) Peak 3 in Figure 2b,c occurs at the same distance in radial space as the low R shoulder found in peak 2 of Figure 2a. Since this shoulder and peak 3 of parts b and c of Figure 2 are immediately adjacent to a much larger peak (labeled 2, 4, and 4 in the three figures, respectively), their actual magnitude is smaller than would be indicated by the peak height. We assume these peaks arise from series termination error in the Fourier transformation or some other mathematical aberration. Regardless, it is necessary to use an R range that encompasses both the principal peak in each (peaks 2, 4, and 4, respectively) and the shoulder or side peaks for successful curve fitting.

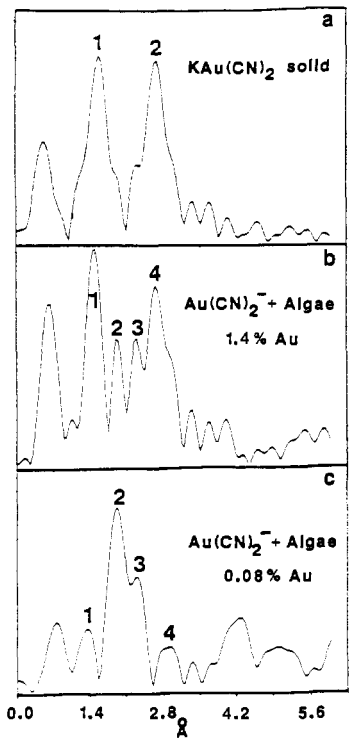

Figure 2. Plots of the modulus of the Fourier transforms vs. radial position (Å) obtained from the EXAFS data of solid $KAu(CN)_2$ with no algae present (a) and the EXAFS data of the samples derived from the reaction of $Au(CN)_2^-$ with algae (b, 1.4% Au; c, 0.08% Au). The changes observed in the FT's indicate that CN may be replaced by S in the Au coordination sphere upon binding to the algae. Peak labels are explained in the text.

peak is a function of the colinearity effect. In addition to these peaks, peak 2 appears at 1.93 Å. This peak position in radial space is at the same position as a typical Au–S absorber–scatterer peak, such as AuSTm. The peak that occurs at ca. 0.6 Å is at too short a distance to be attributed to a Au–scatterer pair. These peaks occur occasionally as a result of the background subtraction. We have found that the low-R peak present in the Fourier transform can be removed with a highly curved quartic spline in the background subtraction. However, under these conditions, the spline no longer represents the smooth background of free-atom absorption. The presence of the low-R peak does not appear to significantly affect the curve-fitting results. Consequently, we prefer to present the data that result from the more realistic data subtraction invoking a cubic spline. Identification of the three peaks, 1 and 2 and the combined peak 3,4, was confirmed by the back-transformation of the data over an R range that encompasses the three peaks of interest. Three-shell curve fitting invoking Au–C,N parameters from $Au(CN)_2^-$ and Au–S parameters provides the best fit of the data. Since EXAFS is unable to distinguish among nearest neighbors in the periodic chart, the Au–S parameters might serve to describe Au–P or Au–Cl backscattering. However, neither of these atoms is likely to be present in a suitable form for chemical binding in the algal biomass. As mentioned previously, sulfur, in the form of free sulfhydryl groups, is a known binding site for gold in biological systems. Consequently, we assign the central peak as an Au–S absorber–scatterer pair. The Au–cyano distances of 2.00 and 3.14 Å for the carbon and nitrogen, respectively, and the Au–S distance of 2.29 Å are consistent with known Au(I)–cyano and Au–S distances.[20]

The coordination numbers calculated for each of the shells seem to be higher than would be expected for a gold(I) two-coordinate species. In general, EXAFS coordination numbers may be accurate to within 15% of the true value. In the case of multishell curve fitting, however, it becomes more difficult to accurately refine the individual amplitude and phase functions, which are used to calculate the coordination number and bond length, respectively. This leads to an overall decrease in the accuracy of both the calculated coordination numbers and bond lengths. In this case, the coordination numbers can do little more than suggest that there is a mixture of gold species present.

Figure 2c is the Fourier transform of the EXAFS data for the sample that contains 0.08% Au. The peaks that correspond to the Au–CN absorber–scatterer pair (peaks 1 and 3,4) have diminished considerably in magnitude and the peak corresponding to the Au–S absorber–scatterer pair has increased in magnitude. Indeed, one of the peaks attributed to the Au–N pair, peak 3, now appears as a shoulder on the Au–S peak, peak 2. The determination of the neighbor atoms was again accomplished by back-transforming an R range that encompasses all of the peaks of interest. The average coordination environment is best described by the three-shell curve fit invoking Au–C,N (from $Au(CN)_2^-$) and Au–S parameters. Though the data are considerably more noisy as a result of the >25-fold decrease in Au concentration in the sample, we are able to see a general increase in the fraction of Au in the sample that is bound to sulfur. Consistent with the previous Au–CN + algae sample, both the calculated Au–S and Au–C distances are in accord with expected values. The Au–N distance of 3.08 Å is shorter than would be expected. As with the problem with the calculated coordination numbers in the previous example, the bond distance error may be the result of the multishell curve-fitting process.

The calculated coordination numbers indicate that a mixture of species is also present for this sample. As expected from the increase in the magnitude of the Au–S peak in the Fourier transform, the calculated coordination number of the Au–S absorber–scatterer pair has increased considerably for this sample from 0.5 to 1.6. This is consistent with a greater percentage of the gold in the sample being bound to sulfur than in the sample that contains 1.4% Au. For the Au–C and Au–N calculated coordination numbers, we would expect approximately equal values if they were to represent a cyano group; however, the EXAFS-calculated coordination numbers are 2.0 for carbon and 0.9 for nitrogen. The larger coordination number for the Au–C pair may indicate that some gold atoms are coordinated to a light-atom scatterer, such as nitrogen or oxygen, since the backscattering amplitude from such a ligand would not be distinguishable from the carbon of cyanide.

Thus, for the general reaction of $Au(CN)_2^-$ with algae, a mixture of species is present and at least some of the gold is bound to sulfur in the algae. Comparison of the results obtained for the 0.08% Au sample with those from the 1.4% Au sample indicates that there is a considerable increase in the relative amount of Au–S coordination in the more dilute sample. This is consistent with the observation that there are sufficient free sulfhydryl groups to account for binding up to ca. 0.1% Au by dry weight of the algae.[4] As the amount of Au binding to the algae is increased, the binding to the sulfhydryl groups is saturated and alternative modes of binding need to be employed. These modes may include both electrostatic interactions of the anionic gold complex with positively charged functional groups as well as substitution of some light atom ligand for cyanide.

$AuCl_4^-$ + Algae. Figure 1 shows the XANES regions of the spectra for the algae samples derived from $AuCl_4^-$. The intense peak found for the solid $Au^{III}Cl_4^-$ (with no algae present) is indicative of the +3 oxidation state. Comparison of the spectrum of solid $KAuCl_4$ with the spectra from the reaction of $AuCl_4^-$ with algae clearly illustrates that algae are able to reduce the Au(III) species to Au(I). The reduced peak height found for the sample that contains 7.5% Au is indicative of a mixture of Au(III) and Au(I) species being present. The sample which contains 0.1% Au exhibits no bound-state transitions in the XANES region. Indeed, the XANES spectrum of the dilute Au–algae sample is very similar in appearance to a typical Au(I) spectrum.

We saw previously that quantitative evidence from the XANES spectrum also exists for the reduction of the Au(III) to Au(I) in these samples. Approximately half of the gold in this sample

(20) Jones, P. G. *Gold Bull.* **1981**, *14*, 102.

remains in the +3 oxidation state and half of the gold in the sample has been reduced to the +1 oxidation state. For the sample that contains 0.1% Au, the inflection point energy occurs at a value that corresponds with a +1 oxidation state. Thus, for relatively low concentrations of gold in the algae, essentially complete reduction of the Au(III) to Au(I) is achieved. The reduction of Au(III) to Au(I) in a biological matrix is consistent with our finding that Au(III) was comprehensively reduced in vivo.[21] Specifically, we found that an acute dose of Au(III) from aqueous $KAuCl_4$ injected into rats led to the formation of gold-containing lysosomal bodies within kidney cells in which the gold oxidation state is +1. It is apparent from the discussion of the XANES region for these samples that reduction of the Au(III) to Au(I) occurs. The fraction of Au(I) present in the sample depends upon the amount of Au(III) initially bound to the algae. The EXAFS analysis on the sample which contains 7.5% Au is also consistent with the finding that a mixture of Au(III) and Au(I) species are present. The curve-fitting analysis indicates that the EXAFS is equally well described by a two-shell Au–S,N or Au–Cl,N fit. The nitrogen shell could also represent an oxygen moiety. The calculated bond lengths for both of these fits, as found in Table II, are consistent with anticipated distances.[20]

Because the available sulfhydryl concentration is too low to account for a significant level of the binding of the gold in this 7.5% Au sample, the Au–Cl,N fit, with 1.2 chlorine atoms and 1.2 nitrogen atoms, probably best describes the average chemical environment around the gold species. This is not to say that some of the Au(I) in the sample does not bind to free sulfhydryls in the algal biomass. On the contrary, from our knowledge of Au(I) species in biological systems, we would expect the Au(I) species to bind to the free sulfhydryl residues. This type of binding, however, would only account for gold levels of about 0.1% by dry weight of the algae.

In addition to demonstrating the coordination of a heavier chlorine-type scatterer, the EXAFS provides conclusive evidence for the coordination of a light-atom scatterer, such as nitrogen or oxygen. The light-atom scatterer may occur from the hydrolysis of the Au(III) species as well as coordination of a gold species to a light atom within the biopolymers. While the EXAFS cannot distinguish between nitrogen coordination to gold over another light-atom scatterer such as oxygen or carbon, previous experimental evidence[4] indicates that at least some of the gold is binding directly to a nitrogen ligand in the biomass. When the algae *C. vulgaris* is treated with succinic anhydride, the amine groups form an amide linkage.[22] The binding capacity of this modified algae for $AuCl_4^-$ was reduced subsequently by 50%.

Thus for the reaction of $AuCl_4^-$ with algae, complex mixtures of gold species result. It is apparent that the algae were capable of reducing the Au(III) to Au(I) in the binding process. Not all of the Au(III) was reduced, however, in the sample that contains 7.5% Au. The EXAFS results on that sample indicate that some of the gold is bound to a light-atom scatterer, probably nitrogen, as well as coordinated to a heavier scatterer. Since there is insufficient sulfhydryl sulfur to account for the coordination number of 1.2, we conclude that most of the heavier scatterer is likely to be chlorine.

Summary. X-ray absorption experiments on these samples have provided significant insight into the nature of the binding of gold from three different starting materials. Strong evidence exists for ligand-exchange reactions leading to formation of bonds between Au(I) and sulfur and/or nitrogen contained in the algae. Once these binding sites are saturated, other modes must be responsible for additional gold uptake by the algae. These include charge interactions between the negatively charged gold complexes with the positvely charged residues in the algae as well as lipophilic interaction between the complexed gold and fatty cellular material. Significantly, the mode of binding appears to be different for the samples derived from the Au(I) complexes than for those derived from $Au(III)Cl_4^-$. There was no evidence for nitrogen coordination in the AuSTm samples. For the samples derived from the cyano complexes, the principal binding atom in the algae appears to be sulfur with vague inference of light-atom coordination in addition to the carbon of the cyano group. For the tetrachloroaurate(III) samples, however, there is clear evidence for light-atom coordination, and this light atom is most likely nitrogen on the basis of other experiments. None of these samples appear to contain gold in the fully reduced Au(0) state, thus indicating that the reduction of Au(III) stops at Au(I) when the samples are lyophilized immediately after short (30 min) incubations.

Acknowledgment. R.C.E. and J.W.W. thank the National Institutes of Health for support (Grant NIH GM35404). D.W.D. and B.G. thank the U.S. Geological Survey and the New Mexico Water Resources Research Institute for financial support and Robert A. McPherson for technical assistance. EXAFS/XANES experiments were conducted at SSRL, which is supported by the Department of Energy, Office of Basic Energy Sciences, and the National Institutes of Health, Biotechnology Resource Program, Division of Research Resources.

Registry No. Au, 7440-57-5; S, 7704-34-9; N_2, 7727-37-9.

Supplementary Material Available: Plots of the raw EXAFS, Fourier transforms, back-transformed EXAFS, and best curve-fit data (26 pages). Ordering information is given on any current masthead page.

(21) Elder, R. C.; Eidsness, M. K.; Heeg, M. J.; Tepperman, K. G.; Shaw, C. F., III; Schaeffer, N. *ACS Symp. Ser.* **1983**, *No. 209*, 385.
(22) Means, G. E.; Feeney, F. E. *Chemical Modification of Proteins*; Holden-Day: San Francisco, CA, 1971.